Evidence for a Plasma Membrane-Mediated Permeability Barrier to Tat Basic Domain in Well-Differentiated Epithelial Cells: Lack of Correlation with Heparan Sulfate†

Stefania Violini,‡ Vijay Sharma,‡ Julie L. Prior,‡ Mary Dyszlewski,‡ and David Piwnica-Worms*,‡,§

Molecular Imaging Center, Mallinckrodt Institute of Radiology, and Department of Molecular Biology and Pharmacology, Washington University School of Medicine, St. Louis, Missouri 63110

Received May 9, 2002; Revised Manuscript Received July 30, 2002

ABSTRACT: Membrane permeation peptides, such as Tat basic domain, have emerged as useful membrane transduction agents with potential utility in therapeutic delivery and diagnostic imaging. While generally thought to universally permeate all cells by a nonselective process, the mechanism of membrane transduction remains poorly characterized. To examine vectorial transport properties of Tat basic domain in well-differentiated epithelial cells possessing tight junctions, L and D stereoisomers of Tat_{48-57} peptide conjugates labeled with ^{99m}Tc were quantitatively analyzed in confluent monolayers of MDCK renal epithelial and CaCo-2 colonic carcinoma cells grown in transwell configurations. In both cell lines, vectorial transepithelial apparent permeability coefficients (P_{app}) for L- and D-[^{99m}Tc]Tat-peptides ranged from 30 to 70 nm/s, comparable to values for the macromolecular impermeant marker inulin in both apical-to-basolateral and basolateral-to-apical directions, but 100-fold less than the P_{app} values for propranolol, a highly permeable control compound. Upon direct instillation of [^{99m}Tc]Tat-peptide into the urinary bladder of living rats in vivo, no transepithelial permeation into other tissues was identified. Furthermore, MDCK and CaCo-2 cells showed a complete lack of intracellular accumulation of fluorescein conjugated Tat-peptide. However, translocation into cells was induced by treatment with plasma membrane permeabilizing agents such as digitonin and acetone/methanol, while cholesterol depletion with β-methyl-cyclodextrin and metabolic inhibition with CCCP or 4 °C showed no effect. By contrast, in Hela and KB 3-1 cells, epithelial lines that do not form tight junctions in monolayer culture, baseline cytoplasmic and nucleolar accumulation was readily observed. Because all four cell lines expressed heparan sulfate proteoglycans, putative receptors for Tat basic peptides, we found no correlation between heparan sulfate and the permeation barrier observed in MDCK and CaCo-2 cells. The unanticipated presence of a permeation barrier to Tat-peptides in well-differentiated epithelial cells suggests the existence of cell-specific mechanisms for mediated translocation of these permeation peptides.

Plasma membranes of cells are generally impermeable to proteins and peptides. The dielectric constant of lipid bilayers imposes a formidable barrier within cell membranes for the diffusive transport of compounds with formal charges or large dipole moments (*1*, *2*). Thus, a variety of highly specialized and regulated systems for mediated secretion of proteins and peptides have evolved in prokaryotic and eukaryotic cells (*3*−*5*), but mechanisms for direct import of proteins and peptides across the plasma membrane from the extracellular spaces to the cytosol are relatively uncharacterized. Nonetheless, several proteins are known to enter cells from the extracellular spaces, including viral transcription factors, plant and bacterial toxins, growth factors and homeoproteins (*6*−*10*). Detailed biochemical analysis has identified specific peptide sequences and domains derived from these proteins that confer surprisingly high membrane permeation properties. These sequences include the third helix of the homeodomain of Antennapedia (*11*), peptides derived from the heavy-chain variable region of an anti-DNA monoclonal antibody (*12*), polyarginines (*13*), and viral transcription factors or derivatives thereof, such as Herpes simplex virus VP22 (*8*), HIV-1[1] Rev and HTLV-1 Rex basic domains (*14*), and HIV-1 Tat protein basic domain (Tat_{47-60}) (*6*, *7*, *15*, *16*).

Little is known regarding the mechanisms of membrane transduction and subcellular localization of these permeation

† This work was supported by grants from the National Institutes of Health (RO1 CA82841 and P50 CA94056).

* Corresponding author. Address: Molecular Imaging Center, Mallinckrodt Institute of Radiology, Washington University School of Medicine, Box 8225, 510 S. Kingshighway Blvd, St. Louis, MO 63110. Tel: (314) 362-9356. FAX: (314)362-0152. E-mail piwnica-wormsd@mir.wustl.edu.

‡ Molecular Imaging Center.

§ Department of Molecular Biology and Pharmacology.

[1] Abbreviations: AHA, aminohexanoic acid; A−B, apical-to-basolateral; B−A, basolateral-to-apical; CCCP, carbonyl-cyanide *m*-chlorophenyl hydrazone; CD, β-methyl-cyclodextrin; DMEM, Dulbecco's modified eagle medium; FM, fluorescein-5-maleimide; HIV, human immunodeficiency virus; HS, heparan sulfate; LEAP, low-energy all-purpose; MDCK, Madin-Darby canine kidney; MEM, minimum essential medium; MEBSS, modified Earle's balanced salt solution; ^{99}Mo, mollibdium-99; P_{app}, apparent permeability coefficient; ^{99m}Tc, technetium-99m; TFA, trifluoroacetate.

10.1021/bi026097e CCC: $22.00
Published on Web 09/27/2002

domains. Whether the mechanisms are general for all permeation peptides or specific for selected proteins or peptides and how cell-specific any targeting mechanism might be remain to be determined. Permeation domains and peptide sequences tend to be highly basic, arginine/lysine-rich, and positively charged at physiological pH. It had been generally thought that the membrane translocation mechanism(s) involve(s) a passive membrane diffusive or destabilization process that does not require binding to cell surface receptors (*10*, *17*). Furthermore, the observation that transduction occurs in many cells at 4 °C has been interpreted to indicate that conventional endocytosis is not involved (*8*, *11*, *18*). Thus, one proposed model for internalization of a prototypic permeation polypeptide, the homeodomain of Antennapedia, is based on the formation of "inverted micelles" (*10*), wherein the peptide recruits negatively charged cell membrane phospholipids to induce formation of a hydrophilic cavity (inverted micelle) which then translocates from the exterior leaflet to the interior leaflet of the plasma membrane depositing peptide into the cytosol. It remains to be determined whether this model is thermodynamically tenable and applies generally to all transduction polypeptides. Indeed, while VP22 holoprotein has been reported to show conformation-dependent membrane interactions under physiological conditions (*19*), cytoskeletal function also has been implicated in penetration of full length VP22 (*8*). In contrast, microtubule- and filament-disrupting agents (colchicine, taxol, nocodozole, and cytochalasin D) are without effect on Tat_{48-57} peptide penetration into human Jurkat cells (*20*). And while endosomotropic agents such as chloroquine and monensin generally are without effect on Tat_{43-60} peptide-mediated transduction, inhibitors of caveolae formation (nystatin and fillipin) inhibit 50% of a luciferase reporter signal arising from Tat_{43-60} peptide-mediated phage penetration in COS-1 cells (*21*). In neurons, low-density lipoprotein receptor-related protein (LRP) has been reported to bind full length Tat protein (*22*), and recent biochemical evidence implicates cell-associated heparan sulfate (HS) proteoglycans as cell receptors for internalization of extracellular full length Tat protein (*23*). HS is ubiquitously expressed on eukaryotic cell membranes and is a major component of basement membranes where the molecule may be involved in the stabilization of other molecules as well as being involved with cell adhesion and glomerular permeability to macromolecules (*24*). HS is polyanionic, and the negative charges could contribute to initial stages of putative absorption and internalization pathways. It also has been suggested that sulfated polysaccharides expressed on HeLa and COS-7 cells could mediate in some manner the translocation of small basic peptides such as Tat_{48-60} and Rev_{34-50} (*25*). In contrast, using HeLa cells, wild-type CHO K1 cells, and CHO mutants deficient in proteoglycan biosynthesis, Silhol et al. (*26*) provide strong evidence that HS proteoglycans are not involved in Tat_{48-60} peptide uptake. Thus, mechanisms of penetration for various permeant peptides and full-length proteins remain to be elucidated.

Specific peptide sequences derived from several of these permeant proteins also have been exploited as vehicles for the transport of various "cargos" such as heterologous proteins, peptides, oligonucleotides, and conjugate compounds into the cell interior of a variety of cells {e.g., refs *10*, *20*, *21*, *27*−*29*}. We recently reported the synthesis of Tat_{48-57} peptides conjugated to peptide-based chelation moieties that enable membrane transduction of radiometals such as technetium-99m (^{99m}Tc) and rhenium-188 (^{188}Re) for use in medical imaging and radiotherapy, respectively (*20*). While the peptide conjugate can conveniently accommodate ^{99m}Tc, a C-terminus cysteine moiety also enables ready conjugation to fluorophores for microscopic analysis of subcellular localization when desired. Radiolabeling with ^{99m}Tc has advantages for quantitative biochemical analysis of cell transport processes both in vitro and in vivo, avoiding confounding complexities associated with fluorescence labeling of compounds (i.e., nonlinear signals, aggregation, and quenching). Synthesized by standard solid-phase methods with either L or D amino acids, these model peptides also enable experiments exploring the stereospecificity of putative mechanisms of peptide permeation.

In the course of investigating biochemical and pharmacokinetic properties of these [^{99m}Tc]Tat-peptides, in vivo imaging experiments in mice indicated that the Tat-peptides were rapidly excreted by the kidneys and retained in the urinary bladder. This prolonged bladder retention implied that the epithelial cells lining the bladder were not penetrated by the Tat-peptide conjugate. Thus, to gain further insight into possible mechanisms of membrane transduction of these Tat-peptides and permeation peptides in general, we investigated more rigorously the membrane transduction properties of Tat-peptides in cells derived from epithelium. Madin-Darby canine kidney (MDCK) epithelial cells represent a model vectorial cell system to study transport mechanisms in distal renal tubule epithelia (*30*). MDCK cells are divided into apical and basolateral membrane domains, each representing functionally and biochemically distinct regions. Moreover, they have been shown to differentiate into columnar epithelium and form tight junctions when cultured on semipermeable membranes. Correspondingly, CaCo-2 cells, a colonic carcinoma cell line, when grown into a confluent monolayer, form tight junctions and express other characteristics of enterocytic differentiation with important morphological and biochemical similarities to small intestinal columnar epithelium (*31*). Both cell lines have been routinely cultured as monolayers on semipermeable membranes for studies of drug transport and compound permeation (*32*, *33*). MDCK and CaCo-2 epithelial cells were found to be impermeant to Tat-peptides.

EXPERIMENTAL PROCEDURES

Materials. MDCK and CaCo-2 cells were obtained from American Type Culture Collection (Rockville, MD). Cell culture media and buffer components were purchased from Gibco BRL (Gaithersburg, MD). Transwell-COL tissue culture inserts (12 mm diameter, 0.4 μm pore size, collagen-coated poly(ethylene terephthalate)) were purchased from Costar Corporation (Cambridge, MA). Fluorescein-5-maleimide was purchased from Molecular Probes, Inc. (Eugene, OR). Antinucleolin primary antibody and rhodamine-conjugated goat antimouse IgG_1 antibody were purchased from Santa Cruz Biotechnology (Santa Cruz, CA). Anti-heparan sulfate primary monoclonal antibody was from Chemicon International, Inc. (Temecula, CA). [Carboxyl-^{14}C]inulin (2.05 mCi/g) and L-[4-^{3}H]propranolol (19 Ci/mmol) were obtained from New England Nuclear (Boston,

MA). All other chemicals were from Sigma Chemical Company (St. Louis, MO).

Preparation of Radiolabeled [^{99m}Tc]Tat-Peptide. Tat-peptide conjugates (Gly-Arg-Lys-Lys-Arg-Arg-Gln-Arg-Arg-Arg-AHA-ϵ-Lys-Gly-Cys, wherein AHA represents an aminohexanoic acid linker) were prepared by solid phase peptide synthesis as previously described (*20*). Peptide stocks (10 mg/mL) were typically prepared in distilled water within 24 h of use. Prior to radiolabeling, peptide purity was confirmed by RP-HPLC analysis utilizing a Vydac C_{18} column (250 × 4.6 mm, 10 μ) and a linear gradient mobile phase starting at 95% solvent A (0.1% TFA) and 5% solvent B (90%:10%, acetonitrile:0.1% TFA) to 40% solvent B over 40 min at a flow rate of 1 mL/min. Preparation and characterization of [^{99m}Tc]Tat-peptide conjugates were accomplished using slight modifications of previously reported procedures (*20*). A commercially available stannous glucoheptonate radiopharmaceutical kit [Sn(II)Cl_2·2H_2O, 0.14 mg; Na glucoheptonate, 200 mg; Glucoscan, DuPont Pharma, Billerica, MA] was reconstituted with 1.0 mL of [^{99m}Tc]Na(TcO_4) (50 mCi) in isotonic saline obtained by eluting a commercial radionuclide ^{99}Mo/^{99m}Tc generator and allowed to stand for 15 min at room temperature. In a small Eppendorf tube, to a 10 μL aliquot of Tat-peptide stock solution were added [^{99m}Tc]-glucoheptonate solution (50−80 μL) and sufficient water to generate a final volume of 100 μL. The reaction was allowed to proceed at 37 °C for 15 min. Radiochemical purity and yields (>95%) of [^{99m}Tc]Tat-peptide complexes were determined by radiometric RP-HPLC (using the same conditions described above) and TLC using silica gel IB2 (J.T. Baker, Inc., Phillipsburg, NJ) developed with either methanol:saline:TFA (68:30:2) or water and analyzed with a scanning radiometric detector (Bioscan, Inc., Washington, DC). By TLC, [^{99m}Tc]Tat complexes remained at the origin in water and moved with the solvent front ($R_f \sim 0.95$) in methanol:saline:TFA. Specific activity was estimated to be 1.84×10^8 mCi/mol.

Cell Cultures. Culture inserts were preincubated with culture medium (1 h, 37 °C) and then seeded with 5×10^5 cells. All cultures were maintained at 37 °C in a 5% CO_2 incubator. MDCK cells were cultured in minimum essential medium (MEM) Earle's salts with 2 mM L-glutamine adjusted to contain 1.5 g/L sodium bicarbonate, 1% nonessential amino acids, 1 mM sodium pyruvate, and 10% fetal bovine serum (FBS). CaCo-2 cells were maintained in Dulbecco's Modified Eagle Medium (DMEM) containing 1% nonessential amino acids, penicillin/streptomycin (0.1%), and 10% heat-inactivated FBS. Media were changed every second day until confluent monolayers formed. KB 3-1 and HeLa cells were cultured in DMEM supplemented with 2 mM L-glutamine, penicillin/streptomycin (0.1%), and 10% heat-inactivated FBS (*34*, *35*).

Transport Assays. While growing in transwells, overall cell morphology was assessed daily by microscopic analysis to determine growth rate and confluence. MDCK and CaCo-2 cells were usually confluent by 2 and 3 weeks in culture, respectively. One hour prior to transwell transport assays, cell monolayers were washed with modified Earle's balanced salt solution (MEBSS) containing (mM) 144 NaCl, 5.4 KCl, 0.8 $MgSO_4$, 0.8 NaH_2PO_4, 1.2 $CaCl_2$, 5.6 glucose, 4.0 Hepes, 1% calf serum, pH 7.4. Transport assays were conducted in MEBSS and initiated upon addition of 0.4 mL of MEBSS to the apical side or 0.6 mL of MEBSS to the basolateral side wherein the initiating solution (cis compartment) contained [^{99m}Tc]Tat-peptide (0.1 mCi/ml; 1 μM total peptide), [^{14}C]inulin (0.25 μCi/ml; 1 μM), and [^{3}H]propranolol (2 μCi/ml; 0.26 μM). [^{14}C]Inulin and [^{3}H]propranolol were used as standards to validate the integrity of the epithelial cell monolayer and document passive transcellular transport, respectively. In selected parallel experiments, carbonyl-cyanide *m*-chlorophenyl hydrazone (CCCP; 5 μM) was added to the buffer solutions. Monolayers were incubated in transport solutions for times up to 120 min at either 37 or 4 °C, and both cis and opposite (trans) compartments were sampled (10 μL) at 5, 15, 30, 60, and 120 min. Solution samples were immediately assayed for γ activity (^{99m}Tc) in a well-type sodium iodide γ counter (Cobra II, Beckman, Downers Glove, IL; 130−165 keV window), allowed to decay for 3 days, and then assayed for beta activity (^{14}C and ^{3}H) in a tabletop β counter (Beckman Coulter, Fuellerton, CA) after solubilizing samples in 5 mL of scintillation solution (Ready Safe Beckman Coulter, Fuellerton, CA). Control experiments with collagen inserts alone confirmed that nonspecific binding of [^{99m}Tc]Tat-peptide, [^{14}C]inulin, and [^{3}H]propranolol to the inserts was <0.18%, 0.03%, and 0.16% of added radioactivity, respectively.

Fluorescence Microscopy. Peptides conjugated with fluorescein maleimide were utilized to directly assess intracellular localization. Peptides were labeled on the C-terminal thiol with fluorescein-5-maleimide (FM) as described previously (*18*, *20*). Exponentially growing MDCK, CaCo-2, KB 3-1, and HeLa cells were seeded onto either eight-well glass chamber slides (Nunc; Naperville, IL), onto 12 mm diameter coverslips, or onto transwell inserts and cultured overnight. Cells were rinsed three times with MEBSS buffer at 37 or 4 °C and then incubated in MEBSS containing FM-Tat-peptide conjugate (0.5−1 μM) at 37 or 4 °C for 20 min. Cells were then fixed at room temperature by direct addition of an equal volume of 8% (v/v) paraformaldehyde in PBS for 10 min, followed by three rinses with PBS. For nucleolin detection, MDCK and CaCo-2 cells were permeabilized with cold (−20 °C) acetone/methanol (1:1) for 10 min, incubated with FM-Tat-peptide conjugate as above, fixed, and then incubated with antinucleolin mAb (2 μg/mL) for 1 h at room temperature. This was followed by incubation in 1.5% horse serum for 1 h and then incubation with rhodamine-conjugated secondary antibody for 45 min. All cells were then washed in PBS and mounted with fluorescence antifading mounting medium following the recommended procedures of the manufacturer (Vector Laboratories, Burlingame, CA). Preparations were analyzed on a Zeiss epifluorescence microscope with a Hamamatsu CCD camera interfaced to a PC (*36*).

Cell Membrane Pretreatments. Cells were grown on coverslips to ~60% confluence, washed in PBS, and then incubated in MEBSS containing digitonin (50 μg/mL) for 30 min at room temperature. To fully permeabilize cell membranes, cells were pretreated with cold acetone/methanol solution (1:1) for 10 min. To deplete membrane cholesterol, cells were washed in serum-free MEM Earle's for MDCK cells or serum-free DMEM for CaCo-2 cells and then incubated in the corresponding serum-free media containing β-methyl-cyclodextrin (15 mM) for 30 min (37 °C in a 5% $C0_2$ incubator). To examine effects of an external protease on peptide uptake, MDCK and CaCo-2 cells were preincu-

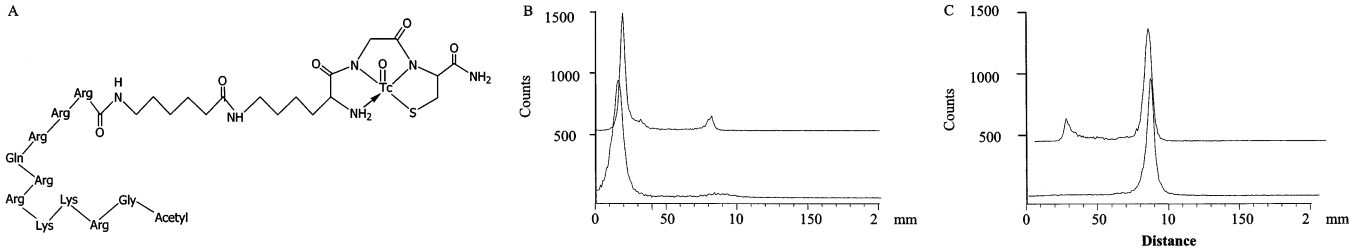

FIGURE 1: (A) Structure of [^{99m}Tc]Tat-peptide complexes. (B, C) Radio-TLC analysis of [^{99m}Tc]Tat-peptide species. TLC chromatograms developed in water (B) or in methanol:saline:TFA (C) of L-[^{99m}Tc]Tat-peptide from stock solution (bottom trace) or from extracellular buffer after 2 h of incubation with MDCK cells at 37°C (top trace). Traces show >90% intact peptide conjugate over the 2 h incubation time.

bated in trypsin−EDTA solution (0.05% − 0.1%) for two minutes (RT). Following each pretreatment, cells were washed with MEBSS buffer and then incubated in MEBSS containing FM-Tat peptide (1 μM) for 20 min at 37 °C, followed by fixation with paraformaldehyde as above. In parallel experiments, after pretreatment of cells with β-methyl-cyclodextrin, lipids were extracted with hexane/2-propanol (3:2, v/v) for 1 h for cholesterol analysis. Cells were then solubilized with 10 mM sodium borate and 1% SDS for determination of total protein by BCA analysis (Pierce Chemical, Rockford, IL) using BSA as a standard. Cholesterol content was determined with a colorimetric assay based on oxidation of cholesterol with cholesterol oxidase (Cholesterol C II kit, Wako Chemicals USA, Richmond, VA) (*37*). Data for cholesterol content were normalized to mg protein and expressed as percent control.

Immunohistochemistry. Cells cultured on glass coverslips were fixed either with 4% paraformaldehyde for 10 min at room temperature or with methanol at −20 °C. After washing in 0.1% Tween-20-PBS, cells were incubated for 30 min (RT) with 1% goat serum in PBS to block nonspecific immunoreactivity. For detection of heparan sulfate proteoglycans, cells were incubated with anti-HS mAb (1:10) for 1 h, then a secondary goat anti-mouse biotinylated IgG antibody (1:200) (Vecstatin ABC kit, Vector Laboratories, Burlingame, CA). All antibodies were diluted in Tween-PBS. After washing, preparations were incubated with streptavidin-horseradish peroxidase, followed by a solution containing 0.1% (w/v) 3-3′-diaminobenzidine-tetrahydrochloride (DAB, Vector Laboratories) and 0.005% (v/v) H_2O_2 at RT for 3 min. Nuclear counterstaining was performed with Mayer hematoxylin for 1 min.

In Vivo Imaging Studies. Female Sprague−Dawley rats (Harlam, Indianapolis, IN) were anesthetized by methoxyflurane inhalation and positioned under a γ scintillation camera (Siemens Basicam, Siemens Medical Systems, Iselin, NJ; LEAP collimator; 20% energy window centered on the 140 keV photopeak of ^{99m}Tc). The urinary bladder was catheterized according to normal animal procedures (*38*). L-[^{99m}Tc]Tat-peptide (1 mCi in 100 μL saline) was instilled into the bladder via the indwelling catheter and the catheter clamped. Sequential posterior images of rats were collected starting immediately after administration of the radiotracer for 5 min each for 30 min. A 256 × 256 image matrix with correction for radioactive decay was used on a PC platform and standard image analysis software. No corrections were made for scatter or attenuation. Whole-body distribution of [^{99m}Tc]Tat-peptide was displayed with gray scale images.

Data Analysis. Values for P_{app} (apparent permeability coefficient; nm/sec) were calculated according to the equation (*32*) $P_{app} = (dQ/dt) \times V_o \times 1/A$, where dQ/dt represents the permeability rate derived from the initial slope (0−60 min) of a plot of radioactivity appearing in the trans compartment (as a percentage of total radioactivity added to the cis (donor) compartment) versus time, V_o is the volume in the cis compartment, and A is the surface area of the filter insert. Data are reported as mean values ± SEM, using the number of replicates for each point as described in figure legends. Pairs were compared by the Student's t test (*39*). Values of $p \leq 0.05$ were considered significant.

RESULTS

L- and D-[^{99m}Tc]Tat-Peptide Characterization. Both L- and D-Tat-peptides (Figure 1A) were analyzed by RP-HPLC to confirm purity prior to radiolabeling. A single major peak was observed with a retention time of 15 min; identity was confirmed by electrospray mass spectrometry (L- and D-Tat-peptide, m/z 1839.0, calcd $C_{74}H_{143}N_{37}O_{16}S_1$, 1839.3). To confirm stability of the [^{99m}Tc]Tat-peptides over the time course of the experiments, radio-TLC was performed on samples obtained from stock solutions after 30 min at 37 °C as well as on aliquots of extracellular space (ECS) buffer obtained both at the beginning and at the end of 2 h of incubation with cells. Initial radiochemical yields were >95%, and both L- and D-[^{99m}Tc]Tat-peptides remained >90% radiolabeled over the time course of the transwell experiments (Figure 1B,C), suggesting the absence of significant transmetalation reactions of both radiotracers during experiments.

Transwell Assays with MDCK and CaCo-2 Cells. Transwell transport assays were performed on MDCK and CaCo-2 cells cultured to confluence on collagen filter inserts. For all transwell experiments, blank inserts and inserts containing cells were used to determine the permeability of [^{99m}Tc]Tat-peptides and radiolabeled reagents. [^{14}C]Inulin, a macromolecular marker, monitored paracellular leak pathways present in the cell monolayer, while [^{3}H]propranolol, known to possess high transcellular permeability across epithelial cells (*33*), was used as a positive control in our transwell system. Only intact monolayers possessing low paracellular fluxes (transepithelial transport of <2%/h of [^{14}C]inulin) were used for further analysis (*36*). For blank inserts, [^{14}C]inulin, [^{3}H]propranolol, and [^{99m}Tc]Tat-peptide each approached plateau levels by 120 min in the trans compartment representing 30−50% of added radioactivity. This was observed in both apical-to-basolateral and baso-

Table 1: Permeability Coefficients for MDCK Cell Monolayers[a]

	P_{app} (nm/sec)							
	[^{99m}Tc]Tat		[^{14}C]inulin		[^{3}H]propranol		ratio [^{99m}Tc]Tat/[^{14}C]In	
	A−B	B−A	A−B	B−A	A−B	B−A	A−B	B−A
L-Tat	31.3 ± 3.5	34.0 ± 4.5	40.3 ± 9.4	24.0 ± 5.1	5320 ± 254[b]	5040 ± 721[b]	0.8 ± 0.2	1.4 ± 0.2
D-Tat	33.3 ± 23.3	123 ± 23.5	72.6 ± 31.8	177 ± 53.3	3256 ± 14.1[b]	2732 ± 371[b]	0.5 ± 0.2	0.7 ± 0.2
L-Tat + CD	66.0 ± 15.5	171 ± 57.2	54 ± 18.3	537 ± 19.1[c]	2560 ± 1074[b]	2340 ± 975[b]	1.1 ± 0.2	0.4 ± 0.1
D-Tat + CD	326 ± 81	207 ± 23.3	408 ± 110	513 ± 239	1612 ± 33.9[b]	4361 ± 165[b]	0.8 ± 0.1	0.5 ± 0.2

[a] Values are the means ± SEM of three experiments under each condition. Statistically significant differences between corresponding A−B and B−A permeability coefficients are indicated: *b*, $p < 0.05$, [^{99m}Tc]Tat vs [^{3}H]propranolol; *c*, $p < 0.05$, [^{99m}Tc]Tat vs [^{14}C]inulin). CD = β-methyl-cyclodextrin; P_{app} = transepithelial apparent permeability coefficient.

Table 2: Permeability Coefficients for CaCo-2 Cell Monolayers[a]

	P_{app} (nm/sec)							
	[^{99m}Tc]Tat		[^{14}C]inulin		[^{3}H]propranol		ratio [^{99m}Tc]Tat/[^{14}C]In	
	A−B	B−A	A−B	B−A	A−B	B−A	A−B	B−A
L-Tat	74 ± 1.4	174 ± 72.1	92 ± 14.1	177 ± 91.2	4944 ± 1040[b]	924 ± 1073[b]	0.8 ± 0.1	1.0 ± 0.2
D-Tat	50 ± 15.5	291 ± 142	174 ± 52.3	342 ± 152	6561 ± 852[b]	8401 ± 940[b]	0.3 ± 0.1	0.9 ± 0.1
L-Tat + CD	48 ± 14.1	111 ± 14.8	210 ± 26.8[c]	180 ± 38.2	5462 ± 74[b]	9403 ± 236[b]	0.3 ± 0.1	0.6 ± 0.1
D-Tat + CD	315 ± 17.6	193 ± 4.9	273 ± 40.3	148 ± 28.6	4976 ± 370[b]	4576 ± 698[b]	1.1 ± 0.5	1.3 ± 0.3

[a] Values are the means ± SEM of three experiments under each condition. Statistically significant differences between corresponding A−B and B−A permeability coefficients are indicated: *b*, $p < 0.05$, [^{99m}Tc]Tat vs [^{3}H]propranolol; *c*, $p < 0.05$, [^{99m}Tc]Tat vs [^{14}C]inulin). CD = β-methyl-cyclodextrin; P_{app} = transepithelial apparent permeability coefficient.

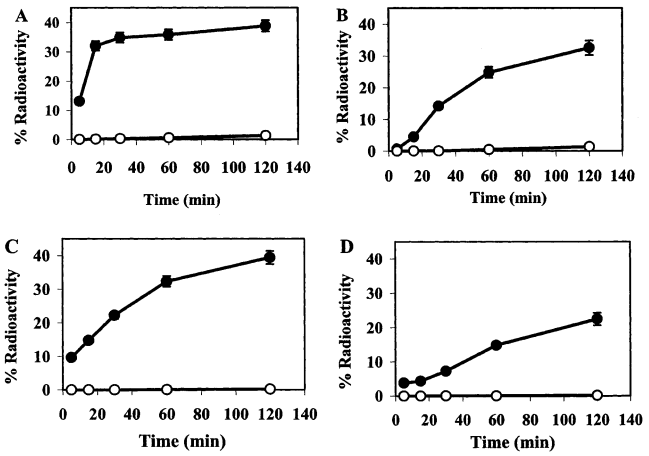

FIGURE 2: Vectorial transport of [^{99m}Tc]Tat-peptide across MDCK (A, B) and CaCo-2 (C, D) cell monolayers. Chambers without cells (●) or with cell monolayers (○) were incubated in MEBSS buffer containing L-[^{99m}Tc]Tat-peptide for the indicated times at 37 °C. Each point represents buffer radioactivity in the trans chamber as a percent of radioactivity added to the cis chamber (mean of triplicate determinations). Bars represent ± SEM when larger than the symbol. Panel A, apical−basolateral (A−B) transport; panel B, basolateral−apical (B−A) transport in MDCK cells. Panel C, A−B transport; panel D, B−A transport in CaCo-2 cells.

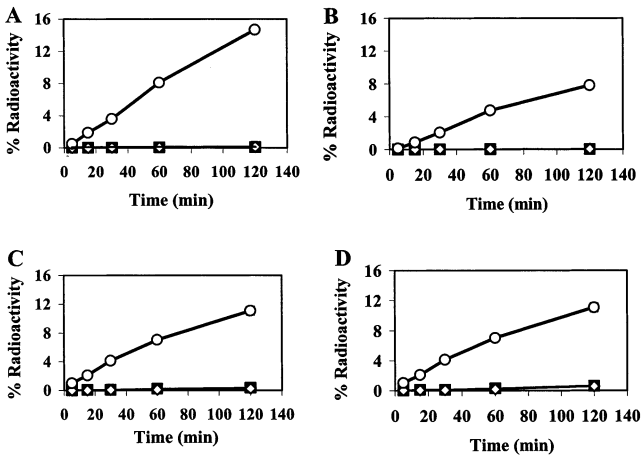

FIGURE 3: Vectorial transport of [^{99m}Tc]Tat-peptide, [^{3}H]propranolol, and [^{14}C]inulin across MDCK (A, B) and CaCo-2 (C, D) cell monolayers. Cells were incubated with MEBSS containing L-[^{99m}Tc]Tat-peptide (◇), [^{3}H]propranolol (○), and [^{14}C]inulin (■) as described under Experimental Procedures. Bars represent ± SEM of triplicate determinations when larger than the symbol. Panels A and B: A−B and B−A transport, respectively. Panels C and D: A−B and B−A transport, respectively.

lateral-to-apical transport experiments, consistent with a freely diffusible bidirectional system in the absence of cells.

In contrast, MDCK and CaCo-2 cells, when grown to confluence on the filter, formed a significant bidirectional diffusion barrier for L-[^{99m}Tc]Tat-peptide. Examples of 2 h transwell transport assays with MDCK and CaCo-2 cells (37°C) are shown in Figure 2 and Figure 3, and apparent permeability coefficients (P_{app}) for L-[^{99m}Tc]Tat-peptide, [^{14}C]-inulin, and [^{3}H]propranolol for each cell line under various conditions are shown in Tables 1 and 2. Pilot data had indicated that D-[^{99m}Tc]Tat-peptides possess 5-fold to 8-fold enhanced accumulation relative to L-[^{99m}Tc]Tat-peptides in human Jurkat cells (*40*), and thus, P_{app} values also were determined for D-[^{99m}Tc]Tat-peptide (Tables 1 and 2). For example, in MDCK cells, P_{app} values for [^{3}H]propranolol were 5320 ± 254 nm/s in the apical-to-basolateral (A−B) direction and 5040 ± 721 nm/s in the basolateral-to-apical (B−A) direction. These were comparable to literature values for [^{3}H]propranolol (*33*), but 170-fold and 150-fold greater, respectively, than the P_{app} values for vectorial permeation of L-[^{99m}Tc]Tat-peptides (A−B, 31.3 ± 3.5; B−A, 34.0 ± 4.5 nm/s). By comparison, values for [^{14}C]inulin, the impermeant control, were 40.3 ± 9.4 and 24.0 ± 5.1 nm/s, respectively, comparable to L-[^{99m}Tc]Tat-peptide values. The L-[^{99m}Tc]Tat-peptide to [^{14}C]inulin P_{app} ratios were close to unity in both directions (0.8 ± 0.2 and 1.4 ± 0.2). Similar results were obtained with D-[^{99m}Tc]Tat-peptide, except that there was a trend for slightly greater B−A permeation (Table

1). Nonetheless, D-[^{99m}Tc]Tat-peptide permeation remained dramatically lower than that of [^{3}H]propranolol under all conditions, and D-[^{99m}Tc]Tat-peptide to [^{14}C]inulin P_{app} ratios remained less than unity in both directions (0.5 ± 0.2 and 0.7 ± 0.2). Identical results were obtained with CaCo-2 cells (Table 2). TLC analysis of buffer samples obtained from both cis and trans compartments each at the beginning and end of selected experiments showed no evidence of significant transmetalation of either L- or D-[^{99m}Tc]Tat-peptides; thus, any differences in transepithelial transport properties could not be attributed to differential transchelation of stereoisomers. In addition, transepithelial permeation for both L- and D-[^{99m}Tc]Tat-peptides remained low when assayed at 4 °C (data not shown), suggesting that the permeation barrier was not highly energy-dependent. Furthermore, the protonophore carbonyl-cyanide *m*-chlorophenyl hydrazone (CCCP; 5 μM), a mitochondrial respiratory uncoupler, had no significant effect on P_{app} of [^{99m}Tc]Tat-peptides (data not shown).

Because agents known to impact cholesterol rafts have been reported to alter cellular uptake of Tat-fusion proteins (*21*), the effect of the cholesterol depleting reagent β-methyl-cyclodextrin was determined. Pretreatment with 15 mM β-methyl-cyclodextrin for 30 min reduced cholesterol content of MDCK and CaCo-2 cells by 38% and 46%, respectively. While β-methyl-cyclodextrin enhanced P_{app} values for both L- and D-[^{99m}Tc]Tat-peptide by 2-fold to 10-fold (Tables 1 and 2), the P_{app} values for [^{14}C]inulin also were enhanced in parallel, thus indicating a concomitant increase in paracellular leak. Thus, no selective increase in [^{99m}Tc]Tat-peptide transwell permeation was observed and the [^{99m}Tc]Tat-peptide to ^{14}C-inulin P_{app} ratios remained ≤ 1 for both MDCK and CaCo-2 cells.

Fluorescence Microscopy. While the tracer experiments advantageously determined vectorial transport of radioactivity in a quantitative manner, the exact subcellular location of [^{99m}Tc]Tat-peptides cannot be evaluated by cell population-based γ-counting techniques. Furthermore, while nonspecific binding of [^{99m}Tc]Tat-peptides to inserts did not affect analysis of transepithelial transport, nonspecific binding (adherence) to filter inserts remained sufficiently high to prohibit quantitative analysis of cell-associated radioactivity. Thus, direct localization of Tat-peptides within MDCK and CaCo-2 cells grown on coverslips was determined by fluorescence microscopy using fluorescein derivatized Tat-peptide conjugates (Figure 4 and Figure 5). For comparison, human KB 3-1 epidermoid carcinoma cells and HeLa cervical carcinoma cells were processed identically. As expected, no cells showed internalization of fluorescein-5-maleimide (FM) when the nonconjugated fluorophore was added to the media or MEBSS alone (data not shown). Furthermore, as previously reported (*20*), KB 3-1 tumor cells showed high levels of fluorescent uptake with a cytoplasmic and focal nuclear pattern after 20 min of exposure to L-FM-Tat peptide (Figure 4H). However, consistent with the lack of transwell permeation, MDCK and CaCo-2 cells did not show any significant internalization of L-FM-Tat peptide under identical conditions. Similarly, D-FM-Tat-peptide was not internalized (data not shown). The lack of FM-Tat-peptide permeation was observed whether the experiments were performed at 37 °C, room temperature, or 4 °C.

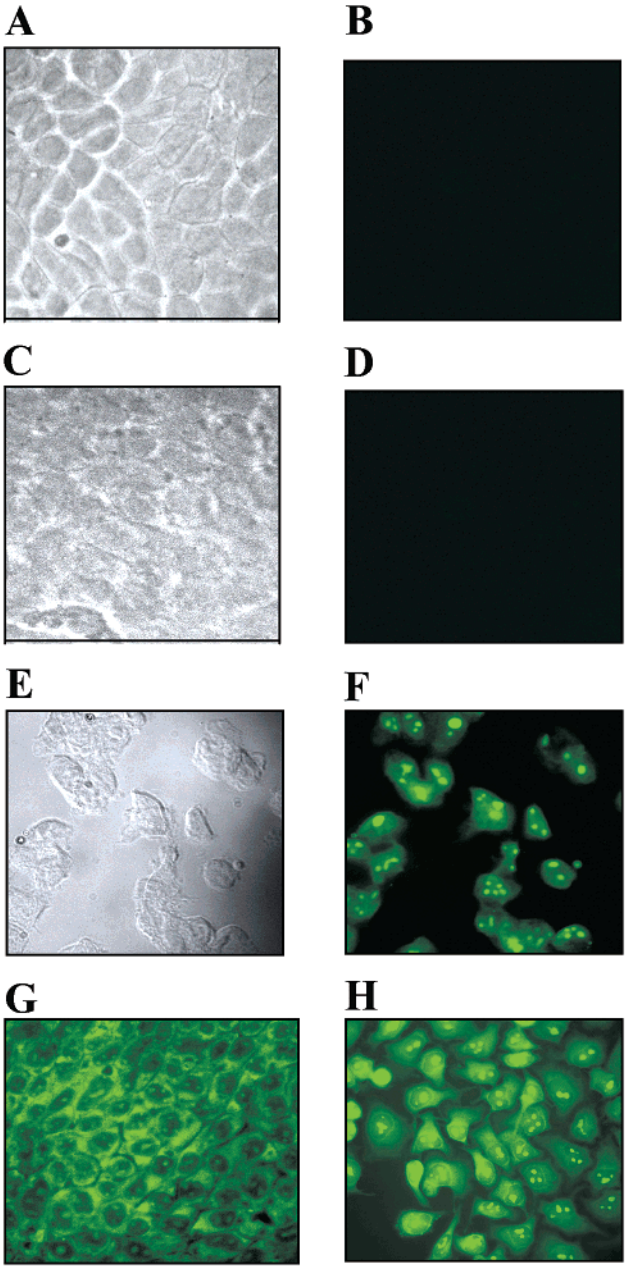

FIGURE 4: Cellular accumulation of fluorescein labeled L-Tat-peptide conjugates in MDCK and KB 3-1 cell lines. Cells in all panels were incubated with FM-Tat-peptide (1 μM) for 30 min at 37 °C followed by fixation. Figure shows bright field (left) and matched fluorescence micrographs (right) of MDCK cells incubated with FM-Tat-peptide alone (panels A and B), after pretreatment with β-methyl-cyclodextrin followed by FM-Tat-peptide (panels C and D), and after pretreatment with digitonin followed by FM-Tat-peptide (panels E and F). MDCK cells after pretreatment with acetone-methanol followed by FM-Tat-peptide (G). KB 3-1 cells incubated with FM-Tat-peptide alone (H). MDCK cells showed FM-Tat-peptide uptake only in the presence of plasma membrane permeabilizing reagents. Magnification: 30×.

Hypothetically, this lack of permeation could be due to a permeation barrier at the level of the plasma membrane, lack of internal binding sites, or lack of putative intracellular translocation mechanisms for Tat-peptides in these cells. To test whether the observed permeation barrier was at the level of the plasma membrane, cells were pretreated for 15−30 min with digitonin (50 μg/mL) and then exposed to FM-Tat-peptides. Digitonin is a mild nonionic detergent that preferentially permeabilizes cholesterol-containing mem-

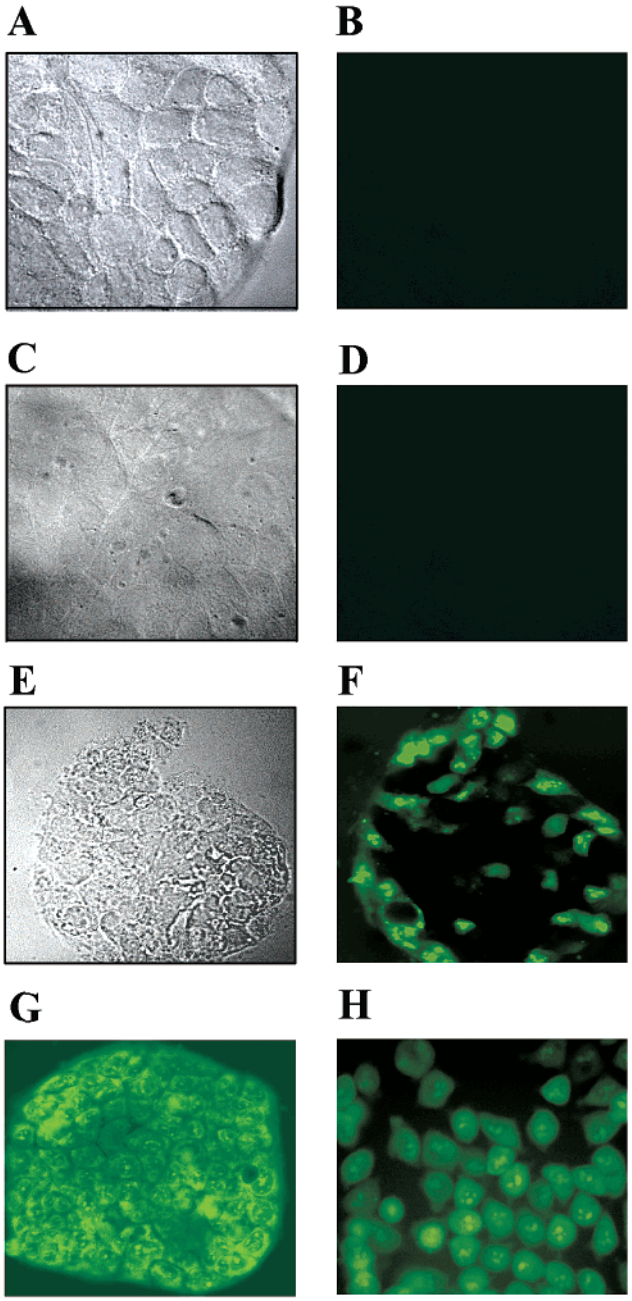

FIGURE 5: Cellular accumulation of fluorescein-labeled L-Tat-peptide conjugates in CaCo-2 and HeLa cells. Cells in all panels were incubated with FM-Tat-peptide (1 μM) for 30 min at 37 °C followed by fixation. Figure shows bright field (left) and matched fluorescence micrographs (right) of CaCo-2 cells incubated with FM-Tat-peptide alone (panels A and B), after pretreatment with β-methyl-cyclodextrin followed by FM-Tat-peptide (panels C and D), and after pretreatment with digitonin followed by FM-Tat-peptide (panels E and F). CaCo-2 cells after pretreatment with acetone-methanol followed by FM-Tat-peptide (**G**). HeLa cells incubated with FM-Tat-peptide alone (H). CaCo-2 cells showed FM-Tat-peptide uptake only in the presence of plasma membrane permeabilizing reagents. Panels A−D, magnification 30×; panels E−H, magnification 20×.

branes and thus is used to selectively permeabilize the plasma membrane (*41*). Interestingly, both MDCK and CaCo-2 cells showed diffuse cytoplasmic and focal nuclear accumulation of the fluorescent peptide when pretreated with digitonin (Figure 4F and Figure 5F, respectively). The overall pattern of accumulation now resembled that observed in KB 3-1 and HeLa cells (Figure 4H and Figure 5H, respectively). Furthermore, when cells were pretreated with cold acetone-methanol, thereby extensively permeabilizing the plasma membrane, bright diffuse cytoplasmic and focal nuclear fluorescence was observed (Figure 4G and Figure 5G). In these experiments, the nuclear component of FM-Tat-peptide was shown to localize within the nucleoli, as confirmed by co-localization of FM-Tat-peptide and an antinucleolin antibody (Figure 6: panels A and B for MDCK cells; panels C and D for CaCo-2 cells). However, in both MDCK or CaCo-2 cells, modest cholesterol depletion with β-methyl-cyclodextrin (15 mM) as above did not enhance uptake of either L-FM-Tat-peptide (Figure 4D and Figure 5D, respectively) or D-FM-Tat-peptide (data not shown). Identical results were obtained whether cells were grown on coverslips or collagen-coated filter inserts (data not shown), providing evidence that the culture substrate was not critical to establishment of the permeation barrier. Similarly, control experiments showed a persistent lack of FM-Tat-peptide uptake at 4°C and also following pretreatment of the cells with trypsin (2 min, RT; data not shown). The latter result would exclude an extracellular protein matrix serving as a physical barrier to Tat-peptide permeation in these cells.

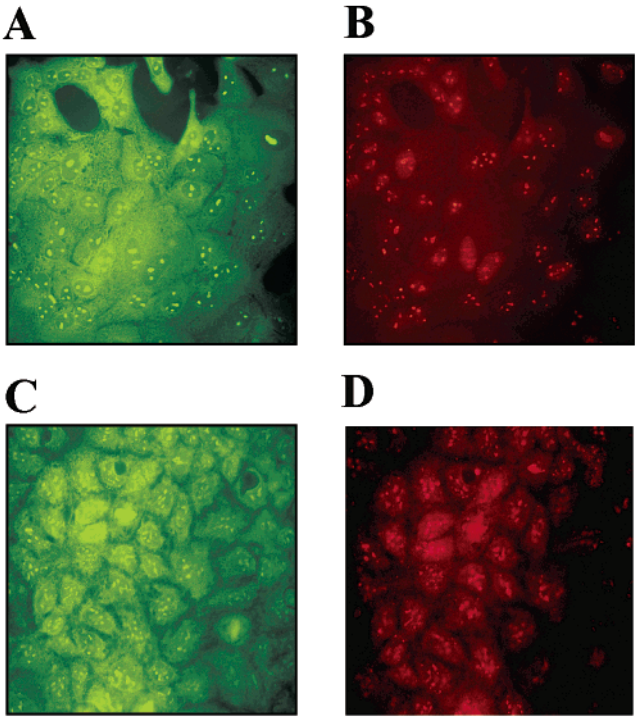

FIGURE 6: L-FM-Tat-peptide localizes to cytosolic and nucleolar compartments in permeabilized cells. Fluorescence micrographs of MDCK (A, B) and CaCo-2 cells (C, D) pretreated with cold acetone−methanol, followed by incubation with FM-Tat-peptide (1 μM) for 60 min, then rhodamine-conjugated antinucleolin mAb. Co-localization of a nucleolar component of FM-Tat-peptide (A, C) and antinucleolin mAb (B, D) is observed in both cell lines. Magnification: 30×.

Heparan Sulfate Expression. To directly explore the potential contribution of HS to uptake and vectorial transport of these Tat-peptides, the expression of HS was determined in MDCK and CaCo-2 cells as well as in KB 3-1 and HeLa cells (Figure 7). Immunohistochemical analysis of HS antigen showed strong positive staining in MDCK and CaCo-2 cells, despite evidence that Tat-peptides did not permeate their plasma membranes. KB 3-1 and HeLa cells also stained highly positive for HS but, in this case, demonstrated high

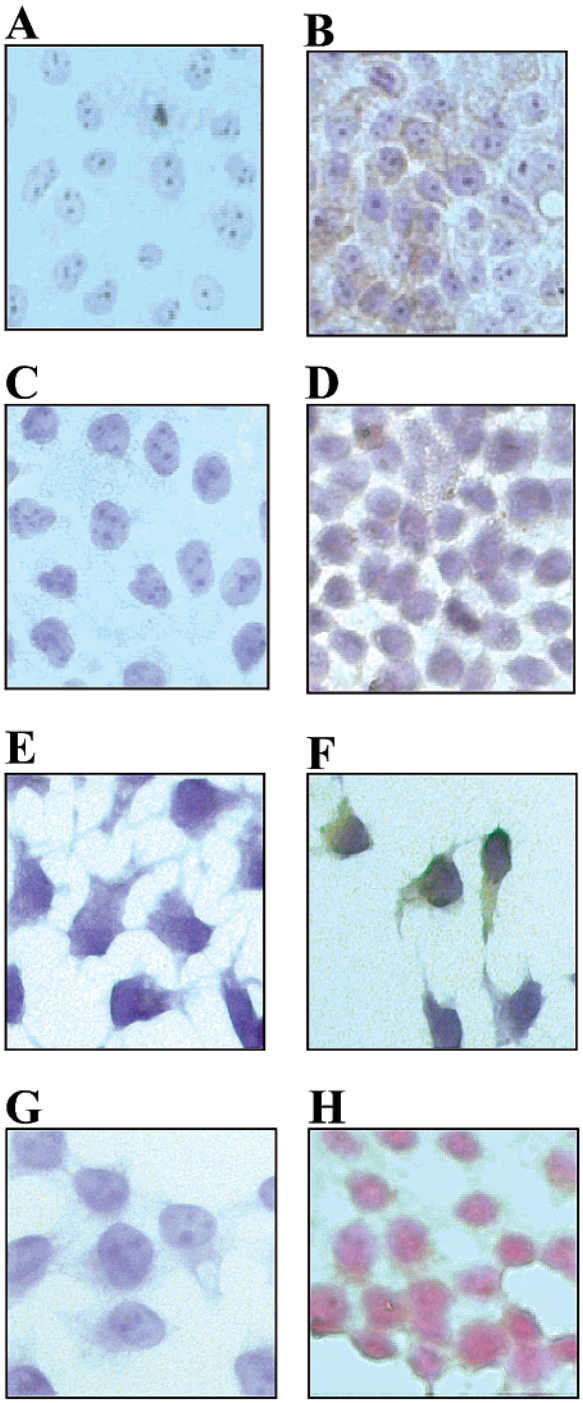

FIGURE 7: Immunohistochemistry for heparan sulfate proteoglycans. Cells were fixed with methanol and processed in the absence or presence of antiheparan sulfate mAb as described under Experimental Procedures. Panels show cells stained in the absence (left, negative control) and presence of primary mAb (right): MDCK cells (A, B); CaCo-2 cells (C, D); KB 3-1 cells (E, F) and HeLa cells (G, H). Magnification: 35x.

Tat-peptide uptake. Thus, HS expression did not correlate with Tat-peptide permeation in these cells.

Imaging a Uroepithelial Transport Barrier in Vivo. Exploiting the 140 keV emission photon of ^{99m}Tc, γ scintigraphy was performed in female rats following catheterization of the urinary bladder and direct instillation of L-[^{99m}Tc]Tat-peptide (1 mCi) into the bladder (Figure 8). In previous experiments, intravenous injection of L-[^{99m}Tc]Tat-peptide resulted in whole-body distribution with focal uptake

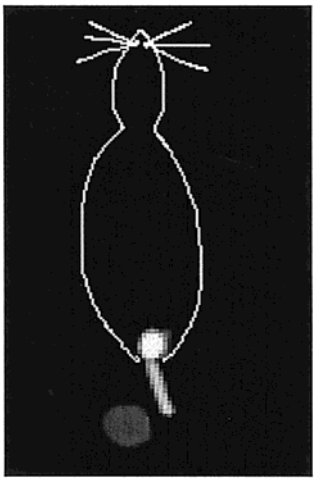

FIGURE 8: Scintigraphic gray scale image of [^{99m}Tc]Tat-peptide retained in the urinary bladder of a catheterized female rat. Following direct bladder instillation of radiolabeled Tat-peptide, posterior images of the rat were obtained with a γ scintillation camera. A representative posterior planar image obtained 30 min postinjection is shown superimposed on an outline of the rat to orient the reader. Radioactivity within the indwelling catheter is seen inferior to the urinary bladder.

in liver and kidneys (*20*). However, following bladder instillation, the complex was observed to remain in the bladder in vivo over the 30 min observation period, showing no distribution throughout the body during the experiment. Prior experiments have confirmed the lack of decomposition of [^{99m}Tc]Tat-peptides in rodent urine (*20*). Scintigraphic techniques are exquisitely sensitive to γ photons, and any transepithelial transport of L-[^{99m}Tc]Tat-peptide across the highly vascular bladder wall would be expected to recirculate to other tissues of the body via the vasculature and be visualized, in particular, within excretory organs such as the liver and kidneys.

DISCUSSION

Peptide-mediated molecular delivery systems have emerged as a powerful tool for protein transduction, translocating heterologous polypeptides across the plasma membrane of a variety of intact cells when added to culture medium. Specific peptide sequences derived from several of these permeant proteins with membrane translocating properties also have been exploited as vehicles for the transport of various substrates such as small peptides, oligonucleotides, and conjugated organic and inorganic compounds into the cell interior of a variety of cells (*10*, *20*, *21*, *27*−*29*). Permeant peptide technology has extensively progressed, leading to an increasing number of distinct sequences utilized to penetrate cells (*13*, *29*). After exogenous application to cultured cells, Tat_{47-57} fusion proteins purified under denaturing conditions are internalized in a rapid, concentration-dependent manner within minutes, and the potential for delivery of proteins in vivo has been demonstrated with B-galactosidase in mouse models (*27*). Early studies suggested that these transduction domains would enable transduction of "cargo" compounds into all cells (*42*), but recently, the universality of the permeation process as a delivery pathway has come under intense scrutiny. For example, it has been reported that intercellular transduction of full-length VP22−GFP fusion proteins in cultured human carcinoma

A549 and H1299 cells as well as monkey COS-1 cells are limited (*43*) and transduction of a Tat_{47-57}−EGFP fusion protein into muscle cells in vivo is poor (*44*). In addition, fusion proteins comprising Tat_{47-57} peptide or full length VP22 linked to the N-terminus of diphtheria toxin A-fragment were found to bind to the surface of Vero cells, but membrane translocation was inefficient (*45*). Whether poor transduction relates to the lack of putative permeation machinery in these cells or conversely, to details of the secondary structure and folded state of specific fusion proteins and cargos, or both remains to be identified.

We now show that MDCK and CaCo-2 cells are impermeant to small Tat-peptides under physiologic conditions to the same degree as the macromolecular marker [^{14}C]inulin. MDCK cells are an immortalized renal tubule epithelial line, while CaCo-2 cells are a transformed intestinal epithelial tumor cell line, and thus, lack of Tat-peptide penetration cannot be ascribed solely to aberrant signal transduction pathways and unregulated cell cycle machinery associated with the transformation process. Transwell transport was analyzed by using both L and D isomers; in both cases, transepithelial permeability was essentially absent. Note that both L- and D-Tat-peptides were not metabolized by cells during the 2 h time course of these experiments as analyzed by radio-TLC. To confirm that Tat-peptides were not able to enter cells, we analyzed by fluorescence microscopy FM-conjugated L- and D-Tat-peptides; both cell lines failed to show any intracellular fluorescence under physiological conditions. The same results were obtained after pretreating MDCK and CaCo-2 cells with trypsin, thereby ruling out any contribution from an extracellular matrix in obstructing Tat-peptide uptake. In contrast, KB 3-1 and HeLa cells, under identical conditions, showed high uptake with a cytosolic and focal nuclear pattern of localization shown immunohistochemically to coincide with nucleoli. The latter observation was consistent with the presence of a nucleolar localizing signal within Tat basic domain (*46*). Interestingly, uptake by FM-labeled peptides was clearly evident in MDCK and CaCo-2 cells after treatment with plasma membrane permeabilizing reagents, such as digitonin and acetone−methanol. Of note, β-methyl-cyclodextrin, a cyclic oligosaccharide reagent that depletes cholesterol and disrupts membrane rafts (*37*), did not stimulate internalization of Tat-peptides, and thus, these data would suggest that cholesterol was not responsible for Tat-peptide exclusion from these cells. Further physiologic confirmation of our results came from in vivo experiments. In rats, radiolabeled [^{99m}Tc]Tat peptide instilled directly into the urinary bladder did not show any redistribution throughout the body, confirming that the Tat-peptide was retained by bladder epithelium in vivo, a uroepithelial tissue of similar embryonic origin as MDCK cells.

Recent papers have also focused on a potential role of HS proteoglycans as receptors for cellular uptake of both full-length Tat protein and small basic peptides. While HS proteoglycans may be involved in internalization of full-length Tat protein fusions (*23*), Silhol et al. (*26*) provide data indicating that HS is not involved in the uptake of small cell penetrating domains such as Tat basic peptide. Of relevance, HS proteoglycans are reported to be expressed in MDCK (*47*, *48*), CaCo-2 (*49*, *50*), and HeLa cells (*51*), and the present study confirmed expression of HS antigen in all these as well as KB 3-1 cells. However, Tat-peptide internalization was identified only in HeLa and KB 3-1 cells. Thus, we conclude that HS proteoglycans are neither sufficient for permeation nor for exclusion of small Tat-peptides from cells.

In sum, this study documented a plasma membrane-mediated permeation barrier to Tat basic peptides in selected well-differentiated epithelial cells, independent of HS proteoglycans, and independent of whether the cells were immortalized or transformed. A possible role for an uncharacterized membrane channel, receptor, or active transporter involved in mediating permeation of Tat-peptides is under investigation.

ACKNOWLEDGMENT

We thank Christina Pica and Delynn Silvestros for technical assistance.

REFERENCES

1. Flewelling, R., and Hubbell, W. (1986) *Biophys. J. 49*, 541−552.
2. Asawakarn, T., Cladera, J., and O'Shea, P. (2001) *J. Biol. Chem. 276*, 38457−38463.
3. Stein, W. (1986) *Transport and Diffusion Across Cell Membranes*, Academic Press, San Diego.
4. Bauer, B., Wolfger, H., and Kuchler, K. (1999) *Biochim. Biophys. Acta 1461*, 217−236.
5. Wagner, C., Lang, F., and Broer, S. (2001) *Am. J. Physiol.: Cell Physiol. 281*, C1077−C1093.
6. Frankel, A., and Pabo, C. (1988) *Cell 55*, 1189−1193.
7. Green, M., and Loewenstein, P. (1988) *Cell 55*, 1179−1188.
8. Elliot, G., and O'Hare, P. (1997) *Cell 88*, 223−233.
9. Falnes, P., and Sandvig, K. (2000) *Curr. Opin. Cell Biol. 12*, 407−413.
10. Prochiantz, A. (2000) *Curr. Opin. Cell Biol. 12*, 400−406.
11. Derossi, D., Calvet, S., Trembleau, A., Brunissen, A., Chassaing, G., and Prochiantz, A. (1996) *J. Biol. Chem. 271*, 18188−18193.
12. Avrameas, A., Ternynck, T., Nato, F., Buttin, G., and Avrameas, S. (1998) *Proc. Natl. Acad. Sc.i U.S.A. 95*, 5601−5606.
13. Wender, P., Mitchell, D., Pattabiraman, K., Pelkey, E., Steinman, L., and Rothbard, J. (2000) *Proc. Natl. Acad. Sci. U.S.A. 97*, 13003−13008.
14. Kubota, S., Siomi, H., Satoh, T., Endo, S., Maki, M., and Hatanaka, M. (1989) *Biochem. Biophys. Res. Comm. 162*, 963−970.
15. Fawell, S., Seery, J., Daikh, Y., Moore, C., Chen, L., Pepinsky, B., and Barsoum, J. (1994) *Proc. Natl. Acad. Sci. U.S.A. 91*, 664−668.
16. Nagahara, H., Vocero-Akbani, A., Synder, E., Ho, A. L., DG, Lissy, N., Becker-Hapak, M., Ezhevsky, S., and Dowdy, S. (1998) *Nat. Med. 4*, 1449−1452.
17. Derossi, D., Chassaing, G., and Prochiantz, A. (1998) *Trends Cell Biol. 8*, 84−87.
18. Vives, E., Brodin, P., and Lebleu, B. (1997) *J. Biol. Chem. 272*, 16010−16017.
19. Kueltzo, L., Normand, N., O'Hare, P., and Middaugh, C. (2000) *J. Biol. Chem. 275*, 33213−33221.
20. Polyakov, V., Sharma, V., Dahlheimer, J., Pica, C., Luker, G., and Piwnica-Worms, D. (2000) *Bioconjugate Chem. 11*, 762−771.
21. Eguchi, A., Akuta, T., Okuyama, H., Senda, T., Yokoi, H., Inokuchi, H., Fujita, S., Hayakawa, T., Takeda, K., Hasegawa, M., and Nakanishi, M. (2001) *J. Biol. Chem. 276*, 26204−26210.
22. Liu, Y., Jones, M., Hingtgen, C., Bu, G., Laribee, N., Tanzi, R., Moir, R., Nath, A., and He, J. (2000) *Nat. Med. 6*, 1380−1387.
23. Tyagi, M., Rusnati, M., Presta, M., and Giacca, M. (2001) *J. Biol. Chem. 276*, 3254−3261.
24. Shriver, Z., Liu, D., and Sasisekharan, R. (2002) *Trends Cardiovasc. Med. 12*, 71−77.
25. Suzuki, T., Futaki, S., Niwa, M., Tanaka, S., Ueda, K., and Sugiura, Y. (2002) *J. Biol. Chem. 277*, 2437−2443.
26. Silhol, M., Tyagy, M., Giacca, M., Lebleu, B., and Vives, E. (2002) *Eur. J. Biochem. 269*, 494−501.
27. Schwarze, S., Ho, A., Vocero-Akbani, A., and Dowdy, S. (1999) *Science 285*, 1569−1572.

28. Josephson, L., Tung, C.-H., Moore, A., and Weissleder, R. (1999) *Bioconjugate Chem. 10*, 186−191.
29. Ford, K., Souberbielle, B., Darling, D., and Farzaneh, F. (2001) *Gene Therapy 8*, 1−4.
30. Gaush, C., Hard, V., and Smith, T. (1966) *Proc. Soc. Exp. Biol. Med. 122*, 931−935.
31. Hidalgo, I., Raub, T., and Borchardt, R. (1989) *Gastroenterology 96*, 736−749.
32. Irvine, J., Takahashi, L., Lockhart, K., Cheong, J., Tolan, W., Selick, H., and Grove, R. (1999) *J. Pharm. Sci. 88*, 28−33.
33. Artursson, P. (1990) *J. Pharm. Sci. 79*, 476−482.
34. Piwnica-Worms, D., Chiu, M., Budding, M., Kronauge, J., Kramer, R., and Croop, J. (1993) *Cancer Res. 53*, 977−984.
35. Luker, G., Sharma, V., Pica, C., Dahlheimer, J., Li, W., Ochesky, J., Ryan, C., Piwnica-Worms, H., and Piwnica-Worms, D. (2002) *Proc. Natl. Acad. Sci. U.S.A. 99*, 6961−6966.
36. Rao, V., Dahlheimer, J., Bardgett, M., Snyder, A., Finch, R., Sartorelli, A., and Piwnica-Worms, D. (1999) *Proc. Natl. Acad. Sci. U.S.A. 96*, 3900−3905.
37. Luker, G., Pica, C., Kumar, A., Covey, D., and Piwnica-Worms, D. (2000) *Biochemistry 39*, 7651−7661.
38. Clair, M., Sowers, A., Davis, J., and LR, R. j. (1999) *Contemp. Top. 8*, 78−79.
39. Glantz, S. A. (1987) *Primer of Biostatistics*, 2nd ed., p 379, Mcgraw-Hill, Inc., New York.
40. Dahlheimer, J., Sharma, V., and Piwnica-Worms, D. (2001) *J. Nucl. Med. 42*, 418S.
41. Hjelmeland, L., and Chrambach, A. (1984) *Methods Enzymol. 1984*, 305−318.
42. Schwarze, S., Hruska, K., and Dowdy, S. (2000) *Trends Cell Biol. 10*, 290−295.
43. Fang, B., Xu, B., Koch, P., and Roth, J. (1998) *Gene Therapy 5*, 1420−1424.
44. Caron, N., Torrente, Y., Camirand, G., Bujold, M., Chapdelaine, P., Leriche, K., Bresolin, N., and Tremblay, J. (2001) *Mol. Ther. 3*, 310−318.
45. Falnes, P., Wesche, J., and Olsnes, S. (2001) *Biochemistry 40*, 4349−4358.
46. Weber, J., Kuo, M., Bothner, B., DiGiammarino, E., Kriwacki, R., Roussel, M., and Sherr, C. (2000) *Mol. Cell Biol. 20*, 2517−2528.
47. Takeuchi, J., Sobue, M., Shamoto, M., Yoshida, M., Sato, E., and Leighton, J. (1977) *Cancer Res. 37*, 1507−1512.
48. Erickson, A., and Couchman, J. (2001) *Matrix Biol. 19*, 769−778.
49. Salmivirta, M., Safaiyan, F., Prydz, K., Andersen, M., Aryan, M., and Kolset, S. (1998) *Glycobiology 8*, 1029−1036.
50. Esclatine, A., Bellon, A., Michelson, S., Servin, A., Quero, A., and Geniteau-Legendre, M. (2001) *Virology 289*, 23−33.
51. Mareel, M., Gragonetti, C., and Dacremont, G. (1979) *Histochemistry 63*, 253−260.

BI026097E